MODELING OF COOL AND BLUE FLAMES AT MULTISTAGE SELF-IGNITION OF n-HEPTANE

V. Ya. Basevich, V. I. Vedeneev, S. M. Frolov, and L. B. Romanovich

N. N. Semenov Institute of Chemical Physics
Russian Academy of Sciences
Moscow, Russia

Introduction

The concepts of low- and high-temperature self-ignition of n-alkane fuels have been introduced into the combustion theory long ago [1, 2]. According to [1, 2], the mechanism of low-temperature self-ignition involves two stages: cool flame and hot explosion. Further progress in understanding the mechanism of low-temperature self-ignition was due to [3] where the concept of multistage self-ignition was proposed. Presented in [3] are the experimental data indicating the existence of the third stage — blue flame — preceding the hot explosion. Characteristic for the blue flame is deeper conversion of a hydrocarbon fuel than in the cool flame. In the blue flame, in addition to the luminescence of excited formaldehyde, HCHO, typical for cool flames, luminescence of formyl, HCO, was normally detected. Experimental data on cool and blue flames propagating in unheated mixtures of acetaldehyde, CH_3CHO, with oxy-

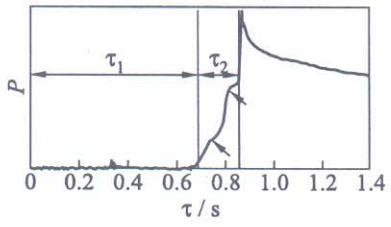

Figure 1 Pressure record at self-ignition of n-heptane–air mixture at $T_0 = 573$ K and $P_0 = 1.5$ atm [9]

gen have been reported in [4]. No systematic study of the encountered phenomena was undertaken since then. Only in 1980s, the interest to the multistage self-ignition was revived in view of its relevance to knock in internal combustion engines [5–7].

This paper deals with the kinetic mechanism of blue flames at the low-temperature self-ignition of *n*-heptane. According to [3, 8, 9], self-ignition of *n*-heptane and *iso*-octane in constant-volume conditions reveals three pressure waves (Fig. 1): first corresponding to cool flame, second to blue flame, and third to hot explosion. Duration of cool and blue flames is the delay of hot explosion denoted as τ_2 in Fig. 1.

Kinetic Mechanism and Results of Calculations

Oxidation of *n*-heptane has been studied in a number of papers. Detailed kinetic mechanisms for complex hydrocarbons like *n*-heptane contain thousands of elementary reactions and hundreds of species. For example, the computer generated mechanism of [10] contains 2400 reactions and 620 species. This mechanism was shown to adequately reproduce the phenomena relevant to both low- and high-temperature self-ignition. However, such mechanisms are too complex and contain too many unknown kinetic parameters to be used for analyses. Therefore, a simplified mechanism of [11] is used herein. The mechanism contains 278 reactions and 39 species. In this mechanism, reactions describing isomerization and decomposition of high-hydrocarbons to low C_1–C_2-hydrocarbons are replaced by several overall reactions with the modeled reaction rate constants. The rest of the mechanism, i.e., a part involving oxidation of C_1–C_2-hydrocarbons, is based on fundamental elementary stages. The mechanism was validated against experimental and computational data within wide ranges of initial temperature (600–1250 K) and pressure (12–100 atm), see, e.g., Fig. 2. The calculations were performed using the computer code NEIKIN providing evolution of temperature and species concentrations at adiabatic constant-volume conditions.

Figure 3 shows the predicted time histories of the normalized temperature (curve *1*) and normalized molar fractions of $C_7H_{15}O_2H$ (*2*), H_2O_2 (*3*), OH (*4*), and H (*5*) in the course of self-ignition of a stoichiometric *n*-heptane–air mixture at initial temperature of $T_0 = 680$ K

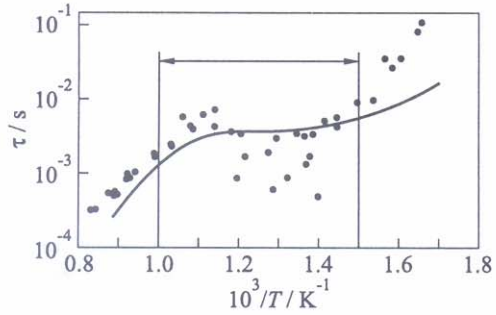

Figure 2 Comparison of predicted (curve) and measured (symbols) ignition delays for a stoichiometric n-heptane–air mixture at $P_0 = 15$ atm [11]. Arrow shows the temperature range of the current study

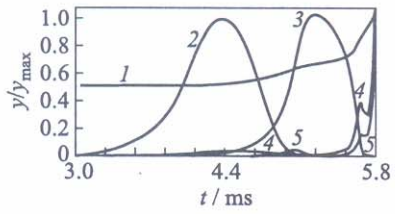

Figure 3 Predicted time histories of the normalized temperature (curve *1*, $y_{max} = 1363$ K) and molar fractions of $C_7H_{15}O_2H$ (curve *2*, $6.2 \cdot 10^{-5}$), H_2O_2 (curve *3*, $5.6 \cdot 10^{-3}$), OH (curve *4*, $2.8 \cdot 10^{-4}$), and H (curve *5*, $1.7 \cdot 10^{-7}$) at self-ignition of a stoichiometric n-heptane–air mixture at $T_0 = 680$ K and $P_0 = 15$ atm

and pressure $P_0 = 15$ atm. Taken as the corresponding reference values are the maximum values of temperature and species molar fractions attained during the calculation. The temperature curve exhibits two clearly observed waves. The first wave originates in the second half of the overall ignition delay and has the amplitude of about 150 K. This wave corresponds to the cool flame. The second wave terminating the ignition delay is considerably shorter than the first wave. Its amplitude is about 250 K. This wave corresponds to the blue flame. After the blue flame, the temperature growth accelerates progressively indicating the beginning of hot explosion. The first — cool flame — stage of the process is caused by thermal decomposition of $C_7H_{15}O_2H$ ($C_7H_{15}O_2H \rightarrow C_7H_{15}O + OH$)

and increasing the overall reaction rate due to the growth of OH concentration (curves *2* and *4* in Fig. 3). The second — blue flame — stage of the process is caused by thermal decomposition of a more stable molecule of hydrogen peroxide, H_2O_2 ($H_2O_2+M \rightarrow OH + OH+M$) and increasing the overall reaction rate due to the growth of OH concentration (curves *3* and *4* in Fig. 3).

Concentration of H atoms (curve *5* in Fig. 3) first slightly increases at the end of the cool flame stage. Then, H concentration increases for the second time simultaneously with the growth of OH concentration caused by H_2O_2 decomposition. Due to complete decomposition of H_2O_2 at the end of the blue flame stage, H and OH concentrations begin to decrease. However, acceleration of chain-branching reaction $H + O_2 \rightarrow OH + O$ leads to a progressive increase in the overall reaction rate resulting in the hot explosion. Maximal temperature tends rapidly to its thermodynamic value (not shown in Fig. 3). Similar inferences have been reported earlier for self-ignition of ethane and acetaldehyde [12, 13].

Figure 4 shows predicted time histories of normalized temperature (*a*) and normalized molar fractions of OH (*b*), H (*c*), H_2O_2 (*d*), and $C_7H_{15}O_2H$ (*e*) at initial pressure $P_0 = 15$ atm and different initial temperatures: $T_0 = 1000$ K (curves *1*), 900 (*2*), 800 (*3*), and 680 K (*4*). The curves in Fig. 4 provide information about the dynamics of *n*-heptane self-ignition in the transition region from multistage to single-stage self-ignition (compare curves *4* and *1*). With increasing the initial temperature, the maximum concentration of $C_7H_{15}O_2H$ decreases by several orders of magnitude and not visible on the scale of Fig. 4*e* (vertical lines *1* and *2* indicate the locations of the corresponding maxima). Contrary to the sharp decrease in the $C_7H_{15}O_2H$ concentration, the decrease in the maximum concentration of H_2O_2 (Fig. 4*d*) is less pronounced. Concentration of atomic hydrogen, H, being quite low during the whole induction period, sharply increases at the hot explosion stage irrespective of the initial temperature.

As the temperature range relevant to $C_7H_{15}O_2H$ formation and decomposition is considerably below than that relevant to H_2O_2 formation and decomposition, the separate appearance of cool and blue flames at *n*-heptane self-ignition is more pronounced than at self-ignition of ethane and, particularly, methane. In the corresponding processes of ethane and methane self-ignition, the main role in cool flame oxidation

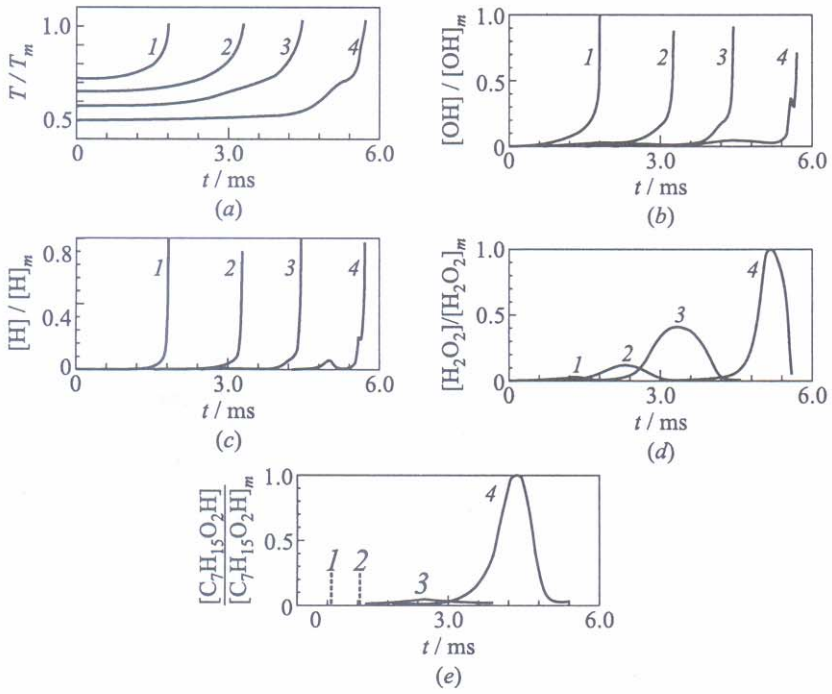

Figure 4 Predicted time histories of normalized temperature (*a*, T_m = 1363 K) and molar fractions of OH (*b*, $[OH]_m = 3 \cdot 10^{-4}$), H (*c*, $[H]_m = 1.3 \cdot 10^{-7}$), H_2O_2 (*d*, $[H_2O_2]_m = 5.6 \cdot 10^{-3}$), and $C_7H_{15}O_2H$ (*e*, $[C_7H_{15}O_2H]_m = 8.2 \cdot 10^{-5}$) at P_0 = 15 atm and T_0 = 1000 K (curves *1*), 900 (*2*), 800 (*3*), and T_0 = 680 K (*4*)

is played by ethyl and methyl hydroperoxides which exhibit stronger coupling with hydrogen peroxide in terms of the characteristic temperature range of formation and decomposition.

Concluding Remarks

Multistage self-ignition of *n*-heptane has been studied computationally based on the kinetic mechanism including several overall reactions of

n-heptane decomposition to C_1–C_2-hydrocarbons and elementary reactions governing their further oxidation. Three stages of the process were distinguished: cool flame, blue flame, and hot explosion. It is inferred that the governing mechanism of cool flame is thermal decomposition of $C_7H_{15}O_2H$ while that of blue flame is thermal decomposition of H_2O_2. Development of hot explosion is mainly due to chain-branching reaction of atomic hydrogen with molecular oxygen. It has been shown that, due to the significant difference in temperatures characteristic to $C_7H_{15}O_2H$ and H_2O_2 formation and decomposition, appearance of cool and blue flames is pronouncedly separated in time before the onset of hot explosion.

Acknowledgments

This work was supported by the Russian Foundation for Basic Research (Grants 02-03-33168 and 02-03-04005) and Federal Program "Integration" (project A0030).

References

1. Shtern, V. Ya. 1960. *Oxidation mechanism of hydrocarbons in gas phase.* Moscow: USSR Academy of Sci. Publ.
2. Lewis, B., and G. Von Elbe. 1961. *Combustion, flames and explosions of gases.* New York: Academic Press.
3. Sokolik, A. S. 1960. *Self-ignition, flame and detonation in gases.* Moscow: USSR Academy of Sci. Publ.
4. Topps, J. E. C., and D. T. A. Townend. 1946. *Trans. Faradey Soc.* 42:345.
5. Ohta, Y., and H. Takahashi. 1983. In: *Flames, lasers, and reactive systems.* Eds. J. R. Bowen, N. Manson, A. K. Oppenheim, and R. I. Soloukhin. Progress in astronautics and aeronautics ser. New York: AIAA Inc. 88:38.
6. Ohta, Y., and H. Takahashi. 1983. In: *Dynamics of flames and reactive systems.* Eds. J. R. Bowen, N. Manson, A. K. Oppenheim, and R. I. Soloukhin. Progress in astronautics and aeronautics ser. New York: AIAA Inc. 95:236.
7. Frolov, S. M., B. E. Gelfand, and S. A. Tsyganov. 1991. Initiation of a detonation wave due to multistage selfignition. In: *Dynamics of detonations and explosions.* Eds. A. L. Kuhl, J.-C. Leyer, A. A. Borisov, and

W. A. Sirignano. Progress in astronautics and aeronautics ser. Washington, DC: AIAA Inc. 133:133.

8. Sokolik, A.S., and S.A. Yantovskii. 1944. *Acta Physicochim. URSS* 19:236.
9. Sokolik, A.S., and S.A. Yantovskii. 1946. *Sov. J. Physical Chemistry* 20:13.
10. Chevalier, C., J. Warnatz, and H. Melenk. 1990. *Ber. Bunsenges. Phys. Chem.* 94:1362.
11. Basevich, V.Ya., S.M. Frolov, *et al.* 1994. *Combustion Explosion Shock Waves* 30(6):15.
12. Basevich, V.Ya., V.I. Vedeneev, and V.S. Arutyunov. 1998. *Chemical Physics Reports* 17(5):73.
13. Basevich, V.Ya., V.I. Vedeneev, and V.S. Arutyunov. 1999. *Chemical Physics Reports* 18(6):40.